Engineering Geology 177 (2014) 25–31

Contents lists available at ScienceDirect

Engineering Geology

journal homepage: www.elsevier.com/locate/enggeo

Technical Note

Post-yield plastic frictional parameters of a rock salt using the concept of mobilized strength

Linjian Ma, Hongfa Xu *, Quan Tong, Lu Dong, Ning Zhang, Jie Li

State Key Laboratory of Disaster Prevention & Mitigation of Explosion & Impact, PLA University of Science and Technology, Nanjing 210007, China

ARTICLE INFO

Article history:
Received 13 June 2013
Received in revised form 4 March 2014
Accepted 13 May 2014
Available online 23 May 2014

Keywords:
Rock salt
Post-yield strength
Mohr–Coulomb criterion
Instantaneous cohesion
Instantaneous friction angle

ABSTRACT

Salt slabbing, spalling and fallout surrounding underground salt storage cavern are closely associated with the nonlinear deformability and post-yield property of rock salt. A better understanding of the pre- and post-yield behavior of rock salt helps the designer in predicting displacements and failure zones around the salt cavity more accurately, as well as in the optimizing design and operation. In the present study, an approach to determine Young's modulus and Poisson's ratio from triaxial test plots has been discussed. A series of compression tests was performed to explore the nonlinear deformability and post-yield strength properties of a rock salt. The rock salt specimens were prepared from Jintan salt deposit, China. It is found that the error in modulus obtained by directly computing the gradient of stress strain curve is relatively small and can be used in analysis. However, error in Poisson's ratio is large. The post-yield strength characteristics were described by nonlinear empirical evolution law of mobilized strength components with maximum principal strain during the process of strain softening/hardening. The proposed generalized Mohr–Coulomb strength criterion with cohesion-weakening and frictional- strengthening was proved effective to capture the post-yield behavior of rock salt.

1. Introduction

Due to very low permeability (10^{-22}–10^{-20} m^2), favorable creep, and damage-healing properties, rock salt is considered a favored medium for underground resource storage and waste disposal. Considerable efforts have been made during the last few decades to explore the mechanical properties of rock salt. It is well established that the short-term deformation and strength characteristics of rock salt are highly dependent on the stress state, loading stress path, strain rate and applied temperature. It has been found that halite lithology shows strain hardening and a strong tendency toward ductile behavior with increasing confining pressure (Liang et al., 2007). The mechanical behavior of rock salt under different stress paths is different. Mikhalyuk et al. (1998), Liang et al. (2011) and Kittitep et al. (2012) concluded that the elastic modulus and compressive strength of rock salt increase with strain and loading rates. The dilatancy boundary depends on both stress loading rate and pore pressure. High pore pressure can accelerate dilatancy (Alkan et al., 2007). Skrotzki (1984) reported that the deformed sodium chloride polycrystals exhibit a sharp transition from brittle to ductile behavior at a certain temperature which depends on the tensile strain rate. The instantaneous strength and strength parameters of rock salt have been mainly studied based on the Mohr–Coulomb strength theory through uniaxial, triaxial compression, tension and direct shear experiments (Farmer and Gilbert, 1984; Hansen et al., 1984; Hunsche, 1984; Hunsche and Albrecht, 1990; Liang et al, 2007). The cohesion and internal friction angle increase with temperature and the strain softening behavior of rock salt becomes increasingly evident (Liang et al., 2006).

The post-yield mechanical characteristics of rock salt play a leading role in short- and long-term salt cavern stability and govern the extent and depth of the breakout (failed or inelastic) zone. Hence, a complete constitutive model is necessary for accurate estimation of stress and displacement distribution in surrounding host salt and capturing the cavern failure mechanism. Rare attempts, however, have been made to assess the post-yield properties of rock salt. Relevant studies mainly focus on the post-peak strain softening properties. For example, Tiwari and Rao (2006) presented equations to estimate post-peak modulus in uniaxial, triaxial and true triaxial stress conditions and a zonation table to assess the strain hardening, softening and plasticity behaviors. Based on the uniaxial and triaxial tests of 80 metamorphic rock specimens (Rajnagar marble, biotite gneiss, augen gneiss and quartzite), post-peak response (e.g., strain softening and residual cohesion) under high confining pressures was analyzed by Kumar et al. (2010).

Traditional approaches of analyzing rock strain-softening behavior are generally based on two popular failure criteria (e.g., Hoek–Brown or Mohr–Coulomb). The criteria assume the simultaneous mobilization of cohesive and frictional strength components (Hoek and Brown, 1980; Itasca, 2005). The softening parameter is commonly defined as a function of internal variables (e.g., plastic shear strain or equivalent plastic strain) or incremental (Vermeer and De Borst, 1984; Itasca, 2001). A method of solving the post-peak stress–strain relationship

* Corresponding author. Tel.: +86 2580826711.
E-mail address: xuhongfa21@163.com (H. Xu).

http://dx.doi.org/10.1016/j.enggeo.2014.05.003
0013-7952/

Table 1
Specimen description for uniaxial and triaxial compressions.

Specimen	Sampling depth/m	Size ($L \times D$)/mm × mm	Unit weight/kN·m^{-3}	Confining conditions/MPa	Test purpose
1	967.50–967.86	102.01 × 52.44	20.416	0	Complete axial stress–strain curve
2	979.20–979.50	101.90 × 50.60	20.415	7	Complete triaxial stress–strain curve
3	995.12–995.47	102.51 × 49.84	20.875	14	
4	960.20–960.72	101.75 × 50.11	20.145	21	
5	1136.51–1136.68	101.94 × 52.26	20.643	7	Elastic portion of triaxial stress–strain curve
6	967.50–967.86	102.18 × 51.86	20.687	7	
7	965.30–965.77	105.48 × 54.63	20.574	7	
8	965.25–965.57	101.78 × 52.56	25.764	7	
9	965.30–965.77	104.28 × 51.61	20.246	14	
10	965.30–965.77	103.22 × 50.64	21.019	14	
11	992.02–992.32	103.78 × 50.19	20.379	14	
12	1045.26–1045.64	102.15 × 51.21	20.903	14	
13	979.20–979.50	102.72 × 50.02	21.413	14	
14	1156.63–1156.84	102.51 × 49.84	20.875	14	
15	1045.26–1045.64	102.70 × 50.86	21.136	21	

was presented by Han et al. (2012) based on the Hoek–Brown strength criterion (Hoek et al., 2002) with strength parameters as a piecewise linear function of a major principal strain. To overcome the shortcomings of previous continuum models with 'c plus $\sigma_n \tan\varphi$' shear strength assumptions in capturing brittle rock spalling or slabbing around underground openings, a bilinear strain dependent cohesion-weakening and frictional-strengthening constitutive model based on the Mohr–Coulomb criterion was pioneered by Hajiabdolmajid (2001), Hajiabdolmajid et al. (2002), and Hajiabdolmajid and Kaiser (2003). A recent comparative study of 'c plus $\sigma_n \tan\varphi$' and 'c then $\sigma_n \tan\varphi$' modeling approaches was demonstrated by Barton and Pandey (2011) for investigating the behavior of multiple mine-stopes in India.

This research aims to experimentally and theoretically assess the elasticity, compressive (yield and peak) strength, and post-yield behavior of Jintan rock salt. A generalized Mohr–Coulomb strength criterion with mobilized cohesion and friction was proposed to describe the strain softening, strain hardening and plastic behavior of rock salt.

2. Test methodology

2.1. Test samples

A set of 15 rock salt samples was obtained from the Tertiary sunken Jintan deposit located at a depth of 900–1200 m underground in China's Jiangsu Province. Among them, one sample was prepared for a uniaxial compression test, and the remaining fourteen samples were used for conventional triaxial compression tests. The Jintan salt specimens mainly consist of 65.7–68.3% NaCl (halite), 4.3–5.9% Na_2SO_4 (sodium sulfate), and 14.5–16.5% $CaSO_4$ (anhydrite), with the remainder of the insoluble part making up 11.5–12.8%. Sample preparation followed the specification for rock tests in water conservancy and hydroelectric engineering (Chinese Industry Standard Editorial Group, 2001) to cut the salt specimens into a standard cylinder with a diameter-to-length ratio of 1:2. The depth of parallelism of the upper and lower faces of the cylinder was controlled between ±0.03 mm with an average diameter of 51.3 mm and an average unit weight of 21.03 kN/m^3.

2.2. Test scheme

Conventional triaxial compression tests were performed at lateral confining pressures of 7 MPa, 14 MPa and 21 MPa and temperature of 25 °C (room temperature) at a constant axial strain-controlled rate of 5×10^{-5} s^{-1}. Both the uniaxial and triaxial compression tests were conducted utilizing a TAW-2000 closed-loop servo-controlled testing machine with a loading rate range of 0.01–50 mm/min and an axial loading capacity up to 2000 kN. The high-pressure triaxial cell is connected to an electric oil pump via a pressure regulator with a loading capacity of 0–100 MPa. The salt samples tested and the scope of testing program are listed in Table 1.

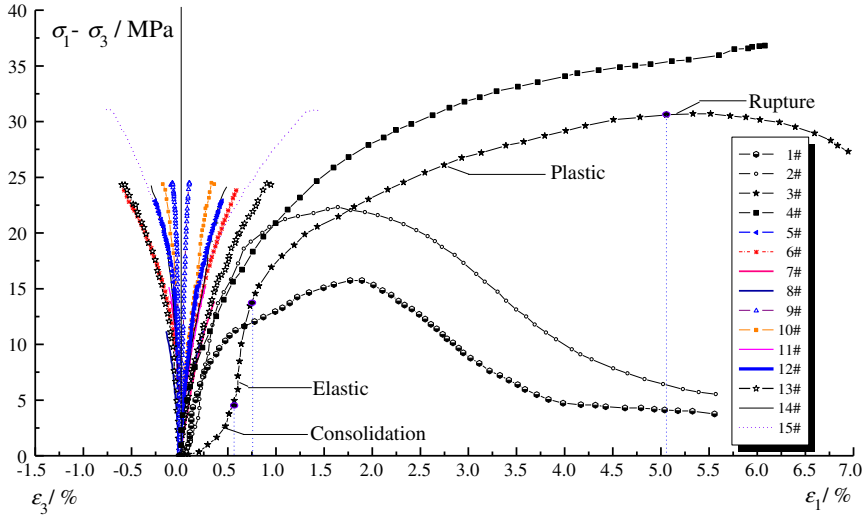

Fig. 1. Stress–strain curves of rock salt specimens under different confining pressures.